Chapter 7

Effects of Surface Forces and Film Elasticity on Froth Stability

Abstract

This chapter describes basic parameters, such as surface forces and film elasticity, affecting the stability of foams (two-phase froths). I used the thin film pressure balance (TFPB) technique to measure the surface forces in foam films stabilized with various frothers such as pentanol, octanol, methyl isobutyl carbinol (MIBC), and polypropylene glycol (PPG). The results were compared with the foam stabilities measured using the shake tests and the film elasticity calculated using the model developed by Wang and Yoon (2006). It was found that at a low electrolyte concentration foam stability is controlled by both film elasticity and surface forces (or disjoining pressure), the relative contributions from each changing with frother concentration and type.

7.1 Introduction

Better understanding of the mechanisms involved in the stability of bubbles and foams is of crucial importance in many scientific and technological fields. In flotation, for example, bubbles laden with hydrophobic particles rise to the surface of a pulp, forming a three-phase foam (froth), which is subsequently removed mechanically or by displacement. The importance in controlling the froth stability in flotation is widely recognized in recent years (1-3).

Many investigators showed that mineral flotation can be described as a first-order process (4,5). In this case, the rate of flotation can be represented by the following relation:

$$\frac{dN}{dt} = -kN \qquad [7.1]$$

where N is the number of floatable (or hydrophobic) particles present in a flotation cell and k is the rate constant. Yoon and Mao (6) showed that

$$k = \frac{1}{4} S_b P \qquad [7.2]$$

where S_b is the superficial surface area rate of bubbles, which is defined as the bubble surface area moving out of the cell per unit time per unit cross-sectional area of the flotation cell under consideration, and P is the probability of the particles being collected by air bubbles. The parameter S_b is given by:

$$S_b = \frac{3V_g}{R_b} \qquad [7.3]$$

where V_g is the superficial aeration rate, which is defined as the volumetric aeration rate normalized by the cross-sectional area of the flotation column, and R_b is the radius of the bubble. Eqs. [7.1-7.3] show that the rate of flotation (k) increases with decreasing bubble size (R_b). In practice, the bubble size in the pulp phase is reduced by adding (non-ionic) surfactants and increasing energy dissipation for bubble generation, while the bubble size in the froth phase is controlled by adjusting froth heights.

It is widely recognized that froth stability may be affected by frother type and concentration, and the presence of solid particles (7-9). The stability of froth (three-phase foam) is closely related to the stability of bubbles and foams (two-phase foams). Foam stability is affected by multiple factors, such as surface tension, film elasticity, and surface forces (10-13). Thermodynamically, air bubbles in water readily coalesce because of the high surface tension (γ=72.6 mJ/m^2), which should give large free energy gains in coalescence. Adding surfactants can lower surface tension, reduce the free energy gains, and hence the probability of coalescence. In flotation, however, the concentrations of surfactants are very low, so that the surface tension changes very little. Laskowski (14) suggested, therefore, that the "static surface tension" may not be directly used to characterize foam stability, and that there is a need to study the effect of "elasticity forces" on foam stability. It has been shown, however, that even the changes in film elasticities are small at frother concentrations employed in flotation practice (12). For

example, the amounts of methyl isobutyl carbinol (MIBC) used in flotation are usually in the range of 0.5- to 1.5×10^{-4} M, in which film elasticities are in the range of 1-2 mN/m only. They found, on the other hand, that the low levels of frother additions cause significant changes in the attractive hydrophobic force, which may be the major destabilizing force for foam films. It was suggested, therefore, that dampening hydrophobic force may be an important role of frother in flotation.

Elasticity, by definition, is the ratio of stress to strain. It is a measure of the property of returning to an initial form or state following deformation. Therefore, the elasticity of foam films is sometimes deemed as the "self-healing" capacity against external disturbance. It is often defined as Gibbs elasticity, the ratio of the change in surface tension to the change in film surface area. Recently, Christenson and Yaminsky (15) derived a simple analytical model for calculate the Gibbs elasticities from surface tension gradients ($d\gamma/dc$). It is a useful model in a sense that the parameter $d\gamma/dc$ can be readily obtained from surface tension isotherm. However, the model does not apply to foam films at low surfactant concentrations because of the simplifying assumptions made for the model derivation (12). Since flotation frothers are typically used at concentrations below 10^{-4} M, Wang and Yoon developed a generalized model that can be applied to foam films at any surfactant concentration.

In the present work, different types of common flotation frothers were used to stabilize the foams. Film elasticities were calculated using the model of Wang and Yoon's (12). In addition, disjoining pressures in foam films have been measured along with equilibrium film thicknesses. The results are discussed to determine the factors affecting foam stabilities.

7.2 Theoretical Model

The elasticity of foam films (E) is defined by Gibbs as follows:

$$E = 2A\frac{d\gamma}{dA} = 2A\frac{d\gamma}{dc}\frac{dc}{dA} \qquad [7.4]$$

where A is the film surface area, and c is the bulk surfactant concentration. For a closed system, the volume of a foam film, $V = AH$, is constant, *i.e.*, dV=0, where H is film thickness. Also, the total number of the surfactant molecules is constant. After several mathematical steps, including using the Gibbs adsorption isotherm, Wang and Yoon (12) derived an expression for E as follows:

$$E = \frac{4RT\Gamma^2}{c(H + 2d\Gamma/dc)} \qquad [7.5]$$

where Γ is the surface excess of a surfactant at an air/water interface. Equation [7.5] is similar to Christenson and Yaminsky's model (15), except that these authors ignored the $d\Gamma/dc$ term, which is significant at low surfactant concentrations. Equation [7.5] can be transformed into a more useful form (12):

$$E = \frac{4RT\Gamma_m^{\,2}K_L^{\,2}c}{H(1 + K_L c)^2 + 2\Gamma_m K_L} \qquad [7.6]$$

by combining it with the Langmuir isotherm:

$$\Gamma = \frac{\Gamma_m K_L c}{1 + K_L c} \qquad [7.7]$$

where Γ_m is the maximum adsorption density, and K_L is the equilibrium adsorption constant.

In calculating E from surface tension data, one should first fit the data to Eq. [7.7] and determine Γ_m and K_L, which can be substituted to Eq. [7.6] to obtain the elasticities. One can also find the maximum value of E at a critical surfactant concentration, c_E^*, as follows:

$$c_E^* = \frac{1}{K_L}\sqrt{1 + \frac{2\Gamma_m K_L}{H}} \qquad [7.8]$$

which can be readily derived by solving $d(1/E)/dc=0$.. If the $2\Gamma_m K_L$ term is much less than H, one obtains that $c_E^* \approx 1/K_L$. Substituting c_E^* for c in Eq. [7.7], one obtains that $\Gamma = 1/2\,\Gamma_m$. Thus, c_E^* represents the surfactant concentration at which Γ is exactly one half of Γ_m. In most cases, c_E^* falls somewhere between $1/K_L$ and the critical micelle concentration (cmc).

7.3 Materials and Experimental Methods

7.3.1 Materials

N-pentanol (99 per cent pure) was obtained from Alfa Aesar. N-octanol (99 per cent pure) and Methyl Isobutyl Carbinol (MIBC) (99 per cent pure) were obtained from Research Chemicals Ltd. The polypropylene glycol with an average molecular weight of 400 (PPG-400) was obtained from Fluka. A high-purity sodium chloride (99.99 per cent pure) from Alfa Aesar was used as an electrolyte. These reagents were used without further purification. All the solutions were prepared using double-distilled and deionized water with a conductivity of 18.2 $M\Omega cm^{-1}$.

7.3.2 Foam Stability Measurement

The stability of three-dimensional foams was measured by the shake tests (13). The tests were conducted using 50 ml volumetric flasks filled with 25 ml of surfactant solution. Each solution was shaken by hand at fixed frequency and time, and was then left to stand. The decay time of the foam was recorded as the time it took for a clear surface to appear at the center of the foam.

7.3.3 Film Thickness Measurement

The thin film pressure balance (TFPB) technique was used to measure the rate of film thinning in a Scheludko cell (16-18). The inner radius of the film holder (r_c) was 2.0 mm. The cell was placed in a vapor-saturated chamber, which was placed on a tilt stage (M-044.00, Polytec PI), which in turn was placed on an inverted microscopic stage (Olympus IX51). The chamber was water-jacketed to maintain the temperature within 23±0.1°C, and the tilt stage was carefully adjusted before each measurement to obtain

horizontal foam films. A PC-based data acquisition system was used to record the intensities of the reflected lights, from which film thicknesses were obtained using the microinterferometric technique (17).

7.4. Results and Discussion

Table 7.1 Various parameters for frothers

Frother	MW (g/mol)	HLB	K_L (M^{-1})	Γ_m ($\mu mol/m^2$)	c_E^* (M)	c_τ^* (M)	$d\tau/dE$ ($sec/mN \cdot m^{-1}$)
Pentanol	88	6.5	55	6	$5.0x10^{-2}$	$3.5x10^{-2}$	3.44
MIBC	102	6.1	230	5	$2.1x10^{-2}$	$3.0x10^{-3}$	1.26
Octanol	130	5.1	2200	8	$8.5x10^{-3}$	$3.2x10^{-4}$	0.19
PPG400	400	9.8	$1.7x10^{6}$	1	$1.1x10^{-4}$	$7.5x10^{-4}$	0.008

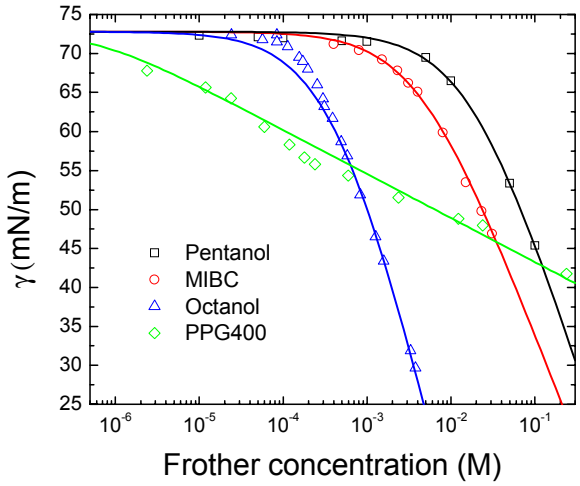

Figure 7.1 Surface tension as a function of frother concentration. The surface tension data of pentanol, MIBC and otanol were adapted from Comley et al (19), while the surface tension isotherm of PPG400 was obtained from Tan et al (20). The solid lines represent the best fits of Lanmguir-Szyszkowski equation (Eq. [7.9]) with the parameters as follows: pentanol, K_L=55 M^{-1}, Γ_m=6 $\mu mol/m^2$; MIBC, K_L =230 M^{-1}, Γ_m =5 $\mu mol/m^2$; octanol, K_L =2200 M^{-1}, Γ_m =8 $\mu mol/m^2$; PPG400, K_L =1.7x106 M^{-1}, Γ_m =1 $\mu mol/m^2$.

Figure 7.1 shows the surface tension isotherms for the frothers studied in the present work. The solid lines represent the Langmuir-Szyszkowski equation:

$$\gamma = \gamma_0 - RT\Gamma_m \ln(1 + K_L c) \qquad [7.9]$$

that has been fitted to the surface tension data reported by Comley et al (19) and Tan et al (20). In the above equation, γ_0 is the surface tension of pure water. The fitting parameters are shown in Table 1 for comparison. In general, K_L increases with increasing molecular weight (MW). This finding suggests that higher molecular weight frothers adsorb more readily at the air/water interface, which in turn suggests that the adsorption

mechanism is driven by entropy changes. On the other hand, the value of Γ_m for PPG-400 is lower than those of the normal alcohols (*i.e.*, pentanol and octanol), which is due to the large molecular weight and hence a large parking area. MIBC also shows a relatively low value of Γ_m, which is due to the branched methyl ($-CH_3$) group, which should create steric hinderence.

Figure 7.2 shows the values of the Gibbs elasticities (E) calculated using Eq. [7.6] as a function of frother concentration. In using Eq.[7.6], the values of H was set equal to the equilibrium thicknesses (H_e), which were in the range of 80-120 nm in the presence of 5×10^{-5} M NaCl, while the values of Γ_m and K_L were obtained by fitting the surface tension data shown in Figure 7.1 to the Langmuir-Szyszkowski equation (Eq.[7.9]). For a given frother, film elasticity increases with increasing frother concentration, reaching a maximum at c_E^*. The values of c_E^* obtained for the different frothers used in the present work are given in Table 1. As shown, c_E^* decreases in the order of pentanol, MIBC, octanol and PPG-400, which is approximately the same order as the increase in K_L. According to Eq. [7.8], c_E^* should be most sensitive to K_L.

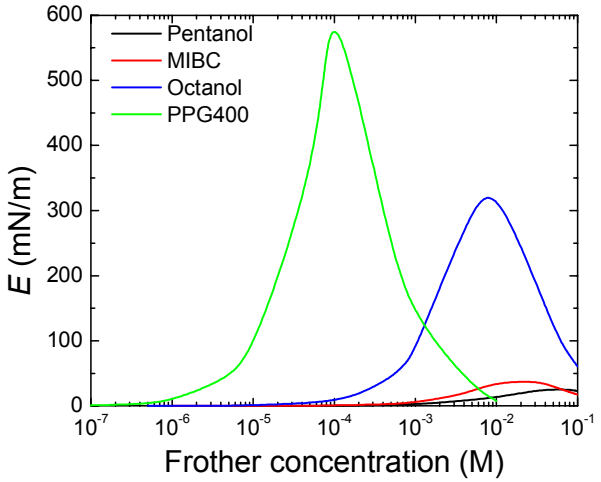

Figure 7.2 Film elasticity (E) calculated using Eq. [7.6] for various frothers: pentanol, MIBC, octanol, and PPG-400. The calculations were made at the equilibrium film thicknesses (H_e), which were in the range of 80-120 nm as measured in the presence of 5×10^{-5} M NaCl.

The following expression is frequently used to calculate the Gibbs elasticity (21-23):

$$E = -\Gamma \frac{d\gamma}{d\Gamma} \qquad [7.10]$$

By combining Eq. [7.10] with Eqs. [7.7] and [7.9], one obtains

$$E = 2RT\Gamma_m K_L c\,. \qquad [7.11]$$

which shows that E should increase monotonically with increasing surfactant concentration (c). The results presented in Figure 7.2 shows, however, that there are maxima for the E vs. c plots. This finding is close to the well-known phenomenon that foams become less stable at surfactant concentrations close to CMC (24). Equations [7.10] and [7.11] show also that E is independent of film thickness, which is obviously an oversimplification. Thus, Eq. [7.6] can give more realistic values of film elasticities.

Note also that film elasticities (E) vary substantially from one frother to another. At 10^{-4} M frother, for example, the values of E for pentanol, MIBC, octanol and PPG400 are 0.14, 0.55, 8.7 and 650 mN/m, respectively. The order of increase in E is the same as increase in K_L, which in turn is related to the molecular weight of the frothers.

In Figure 7.3, the foam stability (τ) measured using the shake tests is plotted versus frother concentration. All the frother solutions were prepared in the presence of $5x10^{-5}$ M NaCl. The results are shown in Figure 7.3. As shown, the foam stability increases with increasing frother concentration, reaching a maximum at a concentration denoted as c_τ^* before decreasing at higher concentrations. The shapes of the curves are similar to those of the E vs. c curves shown in Figure 7.2. However, the values of c_τ^* do not correspond to those of c_E^*, indicating that foam stability does not depend only on the Gibbs elasticity. This discrepancy suggests that there must be other factors affecting foam stability.

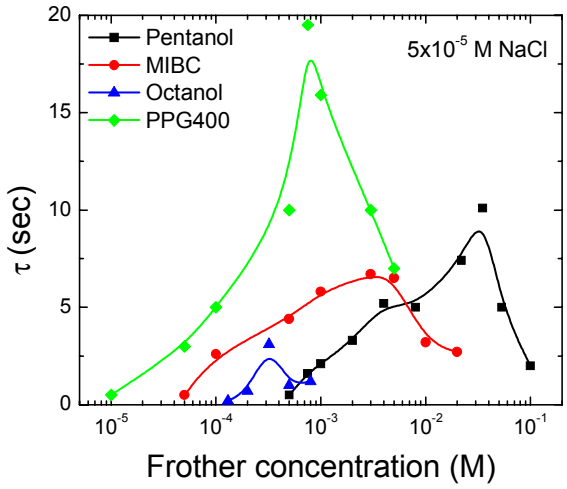

Figure 7.3 Foam stability (τ) as a function of frother concentration.

The foam stabilities (τ) shown in Figure 7.3 are replotted in Figure 7.4 as a function of the film elasticities (E) given in Figure 7.2. Only the data obtained at relatively low frother concentrations, *i.e.*, $<4x10^{-3}$ M for pentanol, $<3x10^{-3}$ M for MIBC, $<3x10^{-4}$ M for octanol, and $<10^{-4}$ M for PPG-400, have been used in this exercise. In flotation, frother concentrations are usually below these concentration limits. Note that for a given frother, the τ vs. E plot is linear. That each plot passes through the origin indicates that in the absence of frother and in the presence of $5x10^{-5}$ M NaCl, the film

elasticity is practically zero and foams are unstable. Note also that the slope of the plot, *i.e.*, dτ/dE, is sensitive to frother type. As shown in Table 1, dτ/dE decreases in the order of pentanol, MIBC, octanol, and PPG-400. If froth stability is determined only by film elasticity, all of the plots should converge into a single curve. That each frother has a unique slope suggests that factors other than the elasticity affect the froth stability. The slope may thus be a reflection of the unique property of a frother. As suggested by Waltermo et al (13) and Wang and Yoon (12), surface forces may be an important factor affecting the foam stability.

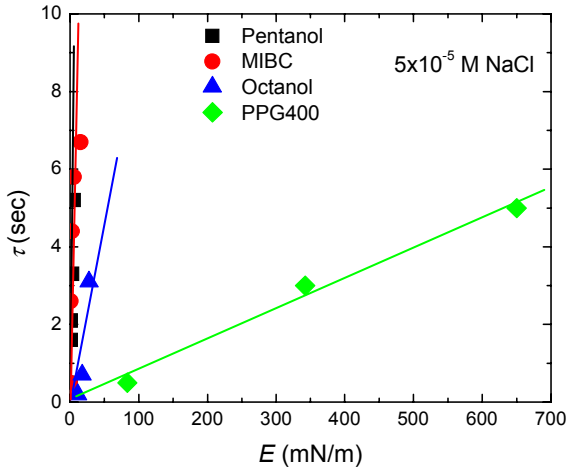

Figure 7.4 Foam stability (τ) as a function of film elasticity (E).

Surface forces affect the pressure in foam films. If the pressure, which is called disjoining pressure (Π), is positive, the film is stable and becomes unstable if the pressure is negative. Thus, the stability of foam films should depend on the surface forces. According to the DLVO theory, the disjoining pressure in a soap film can be expressed as the sum of the double-layer force (Π_{el}) and van der Waals force (Π_{vw}):

$$\Pi = \Pi_{el} + \Pi_{vw} \qquad [7.12]$$

It has been shown, however, that hydrophobic force may also play a role in foam films particularly at low surfactant concentrations (25-28). In this case, Eq. [7.12] may be rewritten as follows:

$$\Pi = \Pi_{el} + \Pi_{vw} + \Pi_{h} \qquad [7.13]$$

At equilibrium, disjoining pressure should be equal to the capillary pressure (P_c), *i.e.*,

$$\Pi = P_c \qquad [7.14]$$

where the capillary pressure is given by the following equation (18),

$$P_c = \frac{2\gamma}{r_c} \qquad [7.15]$$

where γ is surface tension and r_c is the radius of the capillary tube holding a foam film. By using a film holder with r_c = 2 mm, the value of P_c and hence Π in units of N/m^2 should be numerically equal to the surface tension in units of mN/m.

Figure 7.5 shows the values of Π, determined in the manner described above, plotted vs. equilibrium film thickness (H_e). The latter has been measured using the TFPB technique. In general, Π decreases with increasing frother concentration due to the decrease in surface tension (see Eq. [7.15]). At a given H_e, the disjoining pressure decreases systematically in the order of pentanol, MIBC, octanol, and PPG-400. This trend agrees well with the changes in the slope of the straight lines given in Figure 7.4, which strongly indicates that surface forces play a significant role in determining foam stability at relatively low frother concentrations.

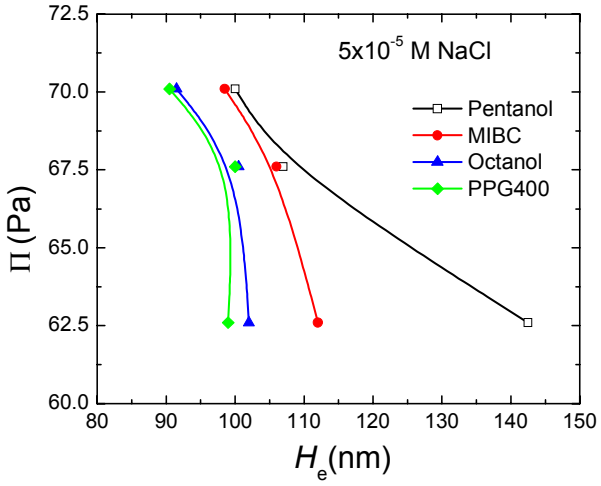

Figure 7.5 Disjoining pressure (Π) as a function of equilibrium film thickness (H_e) at pH 5.6-5.8.

It would be of interest to compare the foam-stabilizing mechanism of PPG-400 to that of MIBC. PPG-400 gave a much lower slope in the foam stability vs. elasticity plot than MIBC did. This finding suggests that the former relies more heavily on elasticity in producing stable foams, while the latter relies on surface forces. This is supported by the fact that MIBC gives higher disjoining pressures than PPG-400, while MIBC has considerably lower film elasticity than PPG-400.

In Figure 7.3, the maximum foam lifetimes (τ_m) are shown. They are 10.1 seconds for pentanol, 6.7 seconds for MIBC, 3.1 seconds for octanol, and 19.5 seconds for PPG-400. It appears that these values are related to the hydrophile-lipophile balance (HLB) numbers of the frothers (see Table 7.1). In general, the higher the HLB number is, the longer the foam life time. Octanol has the lowest HLB value of all the frothers tested in the present work, and has the lowest τ_m. This is not surprising as octanol is widely used in formulating defoaming agents. Many effective defoamers are mixtures of low HLB surfactants, hydrophobic silica particles, and silicone oil. It is possible that the non-ionic surfactants are designed to cause an increase in attractive hydrophobic force and, thereby,

cause a decrease in disjoining pressure (Π). It has recently been shown quantitatively that the role of MIBC in flotation is to dampen the hydrophobic forces associated with air bubbles (12). Waltermo et al (13) also showed that foam stability varies significantly on surface forces.

7.5 Conclusions

Factors affecting the stabilities of the two-phase foams produced in the presence of pentanol, MIBC, octanol and PPG-400 have been studied. It has been found that the stability is affected by both film elasticity and surface forces. The importance of the film elasticity is demonstrated by the linear relationship between foam life time and film elasticity. Also, foam life time approaches zero when film elasticities become zero. On the other hand, the changes in the elasticity due to frother additions are very small at the concentrations typically employed for flotation. Further, plots of the foam life times *vs*. film elasticity vary substantially from one frother to another due to the differences in the surface forces modified by the frother molecules adsorbed at air/water interfaces.

Of the various frothers tested, PPG-400 gave the lowest slope in the foam stability vs. elasticity plot, while pentanol and MIBC gave the highest. This finding suggests that the former relies on elasticity in producing stable foams, while the latter relies on surface forces. This conclusion is also supported by the fact that both pentanol and MIBC give higher disjoining pressures than PPG-400.

7.6 References

1. Neethling, S. J. and Cilliers, J. J., *Int. J. Miner. Process*. 72 (2003) 267.
2. Ata, S., Ahmed, N., and Jameson, G. J., *Int. J. Miner. Process*. 72 (2003) 255.
3. Mathe, Z. T., Harris, M. C., O'Connor, C. T., and Franzidis, J.-P., *Minerals Engineering* 11 (1998) 397.
4. Sutherland, K.L., *J. Phys. Chem*. 52 (1948) 394.
5. Tomlison, H.S. and Fleming, M.G., *Proc. VI Int. Miner. Process. Congr.* 1963, pp.563.
6. Yoon R.-H. and Mao, L., *J. Colloid Interface Sci*. 181 (1996) 613.
7. Darton, R. C. and Sun, K.-H., *Transaction – Institution of Chemical Engineers Part A* 77 (1999) 535.
8. Dippenaar, A., *Int. J. Miner. Process*. 9 (1982) 1.
9. Pugh, R. J., *Adv. Colloid and Interface Sci*. 64 (1996) 67.
10. Langevin, D., *Adv. Colloid and Interface Sci*. 88 (2000) 209.
11. Stubenrauch, C. and Miller, R., *J. Phys. Chem. B* 108 (2004) 6412.
12. Wang, L. and Yoon, R.-H., *Colloids Surfaces A: Physicochem. Eng. Aspects*, in press.
13. Waltermo, Å., Claesson, P. M., Simonsson, S., Manev, E., Johansson, I., and Bergeron, V., *Langmuir* 12 (1996) 5271.

14. Laskowski, J.S., *SME Annual Meeting*, Feb. 23-25, Denver, Colorado, 2004.

15. Christenson, H. K. and Yaminsky, V. V., *J. Phys. Chem*. 99 (1995) 10420.

16. Scheludko, A. and Exerowa, D., *Comm. Dept. Chem., Bul. Acad. Sci*. 7 (1959) 123.

17. Scheludko, A., *Adv. Colloid and Interface Sci*. 1 (1967) 391.

18. Exerowa, D. and Kruglyakov, P. M., *Foam and Foam Films*, Elsevier, 1998.

19. Comley, B. A., Harris, P. J., Bradshaw, D. J., and Harris, M. C., *Int. J. Miner. Process*. 64 (2002) 81.

20. Tan, S.N., Pugh, R.J., Fornasiero, D., Sedev, R., and Ralston, *J., Minerals Engineering* 18 (2005) 179.

21. Bergeron, V., *Langmuir* 13 (1997) 3474.

22. Stoyanov, S., Dushkin, C., Langevin, D., Weaire D., and Verbist, G., *Langmuir* 14 (1998) 4665.

23. Monin, D., Espert, A. and Colin A., *Langmuir* 16 (2000) 3873.

24. Bikerman, J. J., *Foams*, Springer: Heidelberg, Germany, 1973.

25. Yoon, R.-H., Aksoy B. S., *J Colloid Interface Sci*. 211 (1999) 1.

26. Angarska, J. K., Dimitrova, B. S., Danov, K. D., Kralchevsky, P. A., Ananthapadmanabhan, K. P., and Lips, A., *Langmuir* 20 (2004) 1799.

27. Wang, L. and Yoon, R.-H., *Langmuir* 20 (2004) 11457.

28. Wang, L. and Yoon, R.-H., *Colloids Surfaces A: Physicochem. Eng. Aspects* 263 (2005) 267.